

## An Analytical Solution for Coupled Thermoelasticity of Beams Based on Higher-Order Shear Deformation Theory

**M. Abbasi**

*M.Sc. Student,  
 Mechanical Engineering Dept.,  
 Amirkabir University of Technology  
 Tehran, Iran  
 musan.abbasi@gmail.com*

**A. Afshar**

*M.Sc. Student,  
 Mechanical Engineering Dept.,  
 Amirkabir University of Technology,  
 Tehran, Iran  
 arash\_afshar1000@yahoo.com*

**M.R. Eslami**

*Professor,  
 Mechanical Engineering Dept.,  
 Amirkabir University of Technology,  
 Tehran, Iran  
 eslami@aut.ac.ir*

### Abstract

This paper presents an analytical solution using the finite Fourier transformation for coupled thermoelasticity of a beam based on the higher-order shear deformation theory subjected to thermal shock loads. The beam is made of homogenous and isotropic materials. The equation of motion and the conventional coupled energy equation are simultaneously solved to obtain the displacement components and temperature distribution in the beam. Results are presented for simply supported boundary conditions and are verified with those reported in the literature.

**Keywords:** Beams, Coupled thermoelasticity; Higher-order shear deformation theory; Finite Fourier transformation

### Introduction

McQuillen and Brull [1] presented analytical solution for the dynamic thermoelastic response of cylindrical shells using a variational theorem. Coupled thermoelasticity of beams is discussed by Massalas and Kalpakidis [2,3]. The analytical solution of the coupled thermoelasticity of beams with the Euler-Bernoulli assumption is given in [2], and that with Timoshenko assumption is given in [3]. In the treatment of these problems a linear approximation for temperature variation across the thickness direction of the beam is considered. Eslami and Vahedi [4] presented the one-dimensional coupled thermoelasticity problem of rods using the Galerkin finite element method. Finite element coupled thermoelastic analysis of composite Timoshenko-beams is given by Maruthi and Sinha [5], where the temperature variation across the thickness direction is neglected. Manoach and Ribeiro developed a numerical procedure to study the coupled large amplitude thermoelastic vibrations of Timoshenko beams subjected to the thermal and mechanical loads using the finite difference approximation and modal coordinate transformations [6]. The thermoelastic damping of micro-beam is analyzed by Sun et al. [7] using the finite Fourier transformation method combined with Laplace transformation and the normal mode analysis. The governing equations of coupled thermoelastic are established based on the generalized thermoelasticity theory with one relaxation time for simply supported Euler-Bernoulli beam.

This paper presents the behavior of a beam under lateral

thermal shock with coupled thermoelastic assumption. The analysis is based on the finite Fourier transformation method. The beam formulations are based on the higher-order shear deformation theory.

### Derivation of The Governing Equation

Consider a beam of rectangular cross section with length  $l$ , height  $h$  and width  $b$ , as shown in Figure 1. Using the higher-order shear deformation theory, the displacement components are [8]

$$u(x, z, t) = u_0(x, t) + z\psi(x, t) - c'z^3(w_{,x} + \psi), \quad (1)$$

$$w(x, t) = w(x, t).$$

where  $u$  is the axial displacement,  $w$  is the transverse displacement in the  $z$  direction and  $\psi$  is the rotation angle of the cross-section with respect to the longitudinal axis. The constant  $c'$  is given by  $c' = 4/3h^2$ . The subscript zero denotes middle surface and a comma denotes partial differentiation. In terms of the displacement components, the normal and shear strains are given by

$$\varepsilon_x = u_{0,x} + z\psi_{,x} - c'z^3(w_{,xx} + \psi_{,x}), \quad (2)$$

$$\gamma_{xz} = (w_{,x} + \psi) - 3c'z^2(w_{,x} + \psi).$$

Assuming that the beam material is linear elastic and isotropic, the stress-displacement relations for the beam are

$$\sigma_x = E[u_{0,x} + z\psi_{,x} - c'z^3(\psi_{,x} + w_{,xx})] - E\alpha\theta, \quad (3)$$

$$\sigma_{xz} = G[\psi + w_{,x} - 3c'z^2(\psi + w_{,x})].$$

where  $G$  is the shear modulus,  $\alpha$  is the coefficient of thermal expansion,  $\theta = T - T_0$  is the temperature change, and  $T_0$  is the reference temperature, respectively.

We assumed that the temperature change along the height direction is linear. This assumption is justified considering that the thickness of the beam is small with respect to its length [2,3]:

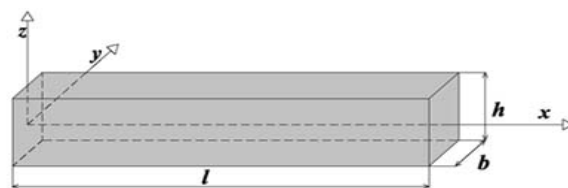


**Figure 1.** The beam and coordinates

$$\theta = \theta_1(x,t) + \frac{z}{h} \theta_2(x,t). \quad (4)$$

where  $\theta_1$  and  $\theta_2$  are unknown to be found through the solution of the coupled equations.

#### Equation of Motion

The equations of motion of a beam based on the higher-order shear deformation theory are [8]

$$N_{,x} = I_0 u_{0,tt} + J_1 \psi_{,tt} - c' I_3 w_{,xtt} \\ \bar{Q}_{,x} + c' P_{,xx} = I_0 w_{,tt} + c' I_3 u_{0,xtt} + J_4 \psi_{,xtt} - c'^2 I_6 w_{,xtt} \quad (5)$$

$$\bar{M}_{,x} - \bar{Q} = J_1 u_{0,tt} + K_2 \psi_{,tt} - J_4 w_{,xtt}$$

where

$$N = \int_z \sigma_x dz, \\ M = \int_z \sigma_x z dz, \\ Q = \int_z \sigma_{xz} dz, \\ P = \int_z \sigma_x z^3 dz, \\ R = \int_z \sigma_{xz} z^2 dz. \quad (6)$$

$$\bar{Q} = Q - 3c'R,$$

$$\bar{M} = M - c'P.$$

$$(I_i) = \int_z \rho z^i dz \quad i = 0,1,\dots,6$$

$$J_i = I_i - c_1 I_{i+2},$$

$$K_2 = I_2 - 2c_1 I_4 + c_1^2 I_6.$$

and  $\rho$  is the mass density of the beam.

Substituting Eqs. (3), (4), and (6) into Eqs. (5), the equations of motion become

$$A_1 u_{0,xx} + A_2 \psi_{,xx} + A_3 w_{,xxx} + A_4 \theta_{1,x} + A_5 \theta_{2,x} + \\ A_6 u_{0,tt} + A_7 \psi_{,tt} + A_8 w_{,xtt} = 0, \\ B_1 u_{0,xxx} + B_2 \psi_{,x} + B_3 \psi_{,xxx} + B_4 w_{,xx} + B_5 w_{,xxx} \\ + B_6 \theta_{1,xx} + B_7 \theta_{2,xx} + B_8 u_{0,xtt} + B_9 \psi_{,xtt} + B_{10} w_{,tt} \\ + B_{11} w_{,xtt} = 0, \quad (7)$$

$$C_1 u_{0,xx} + C_2 \psi + C_3 \psi_{,xx} + C_4 w_{,x} + C_5 w_{,xxx} + \\ C_6 \theta_{1,x} + C_7 \theta_{2,x} + C_8 u_{0,tt} + C_9 \psi_{,tt} + C_{10} w_{,xtt} = 0.$$

where  $A$ 's,  $B$ 's and  $C$ 's are given in Appendix A.

Simply supported boundary conditions are considered for the beam and the beam is assumed to be initially at zero deflection

$$u_{0,x}(0,t) = u_{0,x}(l,t) = 0, \quad t > 0 \\ \psi_{,x}(0,t) = \psi_{,x}(l,t) = 0, \quad t > 0 \\ w(0,t) = w(l,t) = 0, \quad t > 0 \\ u_0(x,0) = \psi(x,0) = w(x,0) = 0. \quad 0 \leq x \leq l \quad (8)$$

#### Energy Equation

The first law of thermodynamics for heat conduction in beam in the coupled form is [4]

$$(k\theta_{,i})_{,i} - \rho c_v \theta_{,t} - \alpha T_0 (3\lambda + 2\mu) (\varepsilon_{ii})_{,i} = 0 \quad (9)$$

where  $k$ ,  $c_v$ ,  $\alpha$ , and  $\varepsilon_{ii}$  are the thermal conductivity, specific heat, coefficient of linear thermal expansion, and normal strain, respectively, and  $\lambda$  and  $\mu$  are the Lamé constants.

The energy equation for the beam based on the higher-order shear deformation theory is reduced to

$$Res = k\theta_{,xx} + k\theta_{,zz} - \rho c_v \theta_{,t} \\ - E\alpha T_0 (u_{0,xt} + z\psi_{,xt} - c'z^3(\psi_{,xt} + w_{,xxt})) = 0 \quad (10)$$

The thermal boundary conditions may be assumed that the lower beam surface is heat isolated and a heat flux  $q(x,t)$  is applied on the upper beam surface. The beam is initially assumed to be at ambient temperature and the thermal boundary and initial conditions are assumed as

$$\theta(0,t) = \theta(l,t) = 0, \quad t > 0 \\ \theta(x,0) = 0. \quad 0 \leq x \leq l \quad (11)$$

Using Eq. (4) and multiplying Eq. (10) by  $dz$  and  $zdz$ , integrating over height  $h$ , the residue  $Res$  of the energy equation may be made orthogonal with respect to  $dz$  and  $zdz$ , to provide two independent equations for two independent functions  $\theta_1$  and  $\theta_2$  as

$$D_1 \theta_{1,xx} + D_2 \theta_{2,xx} + D_3 \theta_{1,t} + D_4 \theta_{2,t} + D_5 u_{0,xt} + \\ D_6 \psi_{,xt} + D_7 w_{,xxt} + D_8 q^-(x,t) + D_9 q^+(x,t) = 0, \\ E_1 \theta_{1,xx} + E_2 \theta_{2,xx} + E_3 \theta_2 + E_4 \theta_{1,t} + E_5 \theta_{2,t} + E_6 u_{0,xt} \\ + E_7 \psi_{,xt} + E_8 w_{,xxt} + E_9 q^-(x,t) + E_{10} q^+(x,t) = 0. \quad (12)$$

where  $q^+$  and  $q^-$  are the applied heat flux on the upper surface and lower surface of the beam, respectively.  $D$ 's and  $E$ 's are given in Appendix A.

#### Solution Procedure

To solve the simultaneous governing equations, dimensionless values are defined as

$$\bar{u}_0 = \frac{k}{q_{avg} \alpha l^2} u_0,$$

$$\bar{\psi} = \frac{k}{q_{avg} \alpha l} \psi,$$

$$\bar{w} = \frac{k}{q_{avg} \alpha l^2} w,$$

$$\bar{\theta} = \frac{k}{q_{avg} \alpha l T_0} \theta,$$

$$\bar{x} = \frac{x}{l},$$

$$\bar{t} = \frac{\kappa t}{h^2}.$$

(13) where  $q_{avg}$  and  $\kappa$  are the average of heat flux and thermal diffusivity, respectively. The bar values indicate dimensionless parameters.

Assuming Eqs. (7) and (12) and using the dimensionless parameters, the five coupled governing equations are

$$a_1 \bar{u}_{0,\bar{x}\bar{x}} + a_2 \bar{\psi}_{,\bar{x}\bar{x}} + a_3 \bar{w}_{,\bar{x}\bar{x}\bar{x}} + a_4 \bar{\theta}_{1,\bar{x}} + a_5 \bar{\theta}_{2,\bar{x}} \\ + a_6 \bar{u}_{0,\bar{t}\bar{t}} + a_7 \bar{\psi}_{,\bar{t}\bar{t}} + a_8 \bar{w}_{,\bar{x}\bar{t}\bar{t}} = 0, \\ b_1 \bar{u}_{0,\bar{x}\bar{x}\bar{x}} + b_2 \bar{\psi}_{,\bar{x}} + b_3 \bar{\psi}_{,\bar{x}\bar{x}\bar{x}} + b_4 \bar{w}_{,\bar{x}\bar{x}} + b_5 \bar{w}_{,\bar{x}\bar{x}\bar{x}} \\ + b_6 \bar{\theta}_{1,\bar{x}\bar{x}} + b_7 \bar{\theta}_{2,\bar{x}\bar{x}} + b_8 \bar{u}_{0,\bar{x}\bar{t}\bar{t}} + b_9 \bar{\psi}_{,\bar{x}\bar{t}\bar{t}} + \\ b_{10} \bar{w}_{,\bar{t}\bar{t}} + b_{11} \bar{w}_{,\bar{x}\bar{x}\bar{t}\bar{t}} = 0, \\ c_1 \bar{u}_{0,\bar{x}\bar{x}} + c_2 \bar{\psi} + c_3 \bar{\psi}_{,\bar{x}\bar{x}} + c_4 \bar{w}_{,\bar{x}} + c_5 \bar{w}_{,\bar{x}\bar{x}\bar{x}} + \\ c_6 \bar{\theta}_{1,\bar{x}} + c_7 \bar{\theta}_{2,\bar{x}} + c_8 \bar{u}_{0,\bar{t}\bar{t}} + c_9 \bar{\psi}_{,\bar{t}\bar{t}} + c_{10} \bar{w}_{,\bar{x}\bar{t}\bar{t}} = 0, \\ d_1 \bar{\theta}_{1,\bar{x}\bar{x}} + d_2 \bar{\theta}_{2,\bar{x}\bar{x}} + d_3 \bar{\theta}_{1,\bar{t}} + d_4 \bar{\theta}_{2,\bar{t}} + d_5 \bar{u}_{0,\bar{x}\bar{t}} \\ + d_6 \bar{\psi}_{,\bar{x}\bar{t}} + d_7 \bar{w}_{,\bar{x}\bar{x}\bar{t}} + d_8 q^- + d_9 q^+ = 0, \\ e_1 \bar{\theta}_{1,\bar{x}\bar{x}} + e_2 \bar{\theta}_{2,\bar{x}\bar{x}} + e_3 \bar{\theta}_2 + e_4 \bar{\theta}_{1,\bar{t}} + e_5 \bar{\theta}_{2,\bar{t}} +$$

$$e_6 \bar{u}_{0,\bar{x}\bar{t}} + e_7 \bar{\psi}_{,\bar{x}\bar{t}} + e_8 \bar{w}_{,\bar{x}\bar{t}} + e_9 q^- + e_{10} q^+ = 0.$$

where  $a$ 's,  $b$ 's,  $c$ 's,  $d$ 's and  $e$ 's are dimensionless constants of coupled equations. Simultaneous solution of these equations provides the distribution of the displacement components of the beam and the temperature variables.

Regarding the boundary conditions in Eqs. (8) and (11), to solve the system of equations of motion and energy equations a finite Fourier transformation can be used as [2,3]

$$\begin{aligned} \bar{u}_{0m}(m,\bar{t}) &= \int_0^1 \bar{u}_0(\bar{x},\bar{t}) \cos(m\pi\bar{x}) d\bar{x}, \\ \bar{\psi}_m(m,\bar{t}) &= \int_0^1 \bar{\psi}(\bar{x},\bar{t}) \cos(m\pi\bar{x}) d\bar{x}, \\ \bar{w}_m(m,\bar{t}) &= \int_0^1 \bar{w}(\bar{x},\bar{t}) \sin(m\pi\bar{x}) d\bar{x}, \\ \bar{\theta}_{1m}(m,\bar{t}) &= \int_0^1 \bar{\theta}_1(\bar{x},\bar{t}) \sin(m\pi\bar{x}) d\bar{x}, \\ \bar{\theta}_{2m}(m,\bar{t}) &= \int_0^1 \bar{\theta}_2(\bar{x},\bar{t}) \sin(m\pi\bar{x}) d\bar{x}. \end{aligned} \quad (15)$$

where  $m=1,3,5,\dots$

The solutions given by Eqs. (15) automatically satisfy the boundary conditions (i.e., Eqs. (8) and (11)). Based on the Fourier series theory, the inverse transformation of Eqs. (15) are expressed by

$$\begin{aligned} \bar{u}_0(\bar{x},\bar{t}) &= 2 \sum_m \bar{u}_{0m}(m,\bar{t}) \cos(m\pi\bar{x}), \\ \bar{\psi}(\bar{x},\bar{t}) &= 2 \sum_m \bar{\psi}_m(m,\bar{t}) \cos(m\pi\bar{x}), \\ \bar{w}(\bar{x},\bar{t}) &= 2 \sum_m \bar{w}_m(m,\bar{t}) \sin(m\pi\bar{x}), \\ \bar{\theta}_1(\bar{x},\bar{t}) &= 2 \sum_m \bar{\theta}_{1m}(m,\bar{t}) \sin(m\pi\bar{x}), \\ \bar{\theta}_2(\bar{x},\bar{t}) &= 2 \sum_m \bar{\theta}_{2m}(m,\bar{t}) \sin(m\pi\bar{x}). \quad m=1,3,\dots \end{aligned} \quad (16)$$

Applying the Fourier transformations to Eqs. (14) and the initial conditions Eqs. (8) and (11) leads to

$$\begin{aligned} -r^2 a_1 \bar{u}_{0m} - r^2 a_2 \bar{\psi}_m - r^3 a_3 \bar{w}_m + r a_4 \bar{\theta}_{1m} + r a_5 \bar{\theta}_{2m} \\ + a_6 \bar{u}_{0m,\bar{t}\bar{t}} + a_7 \bar{\psi}_{m,\bar{t}\bar{t}} + a_8 \bar{w}_{m,\bar{t}\bar{t}} = 0, \\ r^3 b_1 \bar{u}_{0m} - r b_2 \bar{\psi}_m + r^3 b_3 \bar{w}_m - r^2 b_4 \bar{w}_m + r^4 b_5 \bar{w}_m \\ - r^2 b_6 \bar{\theta}_{1m} - r^2 b_7 \bar{\theta}_{2m} - r b_8 \bar{u}_{0m,\bar{t}\bar{t}} - r b_9 \bar{\psi}_{m,\bar{t}\bar{t}} + \\ b_{10} \bar{w}_{m,\bar{t}\bar{t}} - r^2 b_{11} \bar{w}_{m,\bar{t}\bar{t}} = 0, \\ -r^2 c_1 \bar{u}_{0m} + c_2 \bar{\psi}_m - r^2 c_3 \bar{w}_m + r c_4 \bar{w}_m - r^3 c_5 \bar{w}_m + \\ r c_6 \bar{\theta}_{1m} + r c_7 \bar{\theta}_{2m} + c_8 \bar{u}_{0m,\bar{t}\bar{t}} + c_9 \bar{\psi}_{m,\bar{t}\bar{t}} + r c_{10} \bar{w}_{m,\bar{t}\bar{t}} = 0, \\ -r^2 d_1 \bar{\theta}_{1m} - r^2 d_2 \bar{\theta}_{2m} + d_3 \bar{\theta}_{1m,\bar{t}} + d_4 \bar{\theta}_{2m,\bar{t}} - r d_5 \bar{u}_{0m,\bar{t}} \\ - r d_6 \bar{\psi}_{m,\bar{t}} - r^2 d_7 \bar{w}_{m,\bar{t}} + (2d_8/r) q^- + (2d_9/r) q^+ = 0, \\ -r^2 e_1 \bar{\theta}_{1m} - r^2 e_2 \bar{\theta}_{2m} + e_3 \bar{\theta}_{2m} + e_4 \bar{\theta}_{1m,\bar{t}} + e_5 \bar{\theta}_{2m,\bar{t}} - \\ r e_6 \bar{u}_{0m,\bar{t}} - r e_7 \bar{\psi}_{m,\bar{t}} - r^2 e_8 \bar{w}_{m,\bar{t}} + (2e_9/r) q^- \\ + (2e_{10}/r) q^+ = 0. \quad r = m\pi \end{aligned} \quad (17)$$

The system of coupled Eqs. (17) are functions of the Fourier parameter  $m$  and time  $t$ . The solution presented in this paper is obtained by the finite Fourier transformation, where time is eliminated using the Laplace transform. Once the solution in space domain is obtained, an analytical scheme is used for the Laplace

transform to find the final solution in real time domain. Assuming the lower beam surface is heat isolated ( $q^- = 0$ ) and a step function heat flux  $q^+$  is applied on the upper beam surface and applying the Laplace transform to Eqs. (17), give

$$\begin{aligned} -r^2 a_1 U_{0m} - r^2 a_2 \Psi_m - r^3 a_3 W_m + r a_4 \Theta_{1m} \\ + r a_5 \Theta_{2m} + a_6 s^2 U_{0m} + a_7 s^2 \Psi_m + a_8 s^2 W_m = 0, \\ r^3 b_1 U_{0m} - r b_2 \Psi_m + r^3 b_3 \Psi_m - r^2 b_4 W_m + r^4 b_5 W_m \\ - r^2 b_6 \Theta_{1m} - r^2 b_7 \Theta_{2m} - r b_8 s^2 U_{0m} - r b_9 s^2 \Psi_m + \\ b_{10} s^2 W_m - r^2 b_{11} s^2 W_m = 0, \\ -r^2 c_1 U_{0m} + c_2 \Psi_m - r^2 c_3 \Psi_m + r c_4 W_m \\ - r^3 c_5 W_m + r c_6 \Theta_{1m} + r c_7 \Theta_{2m} + c_8 s^2 U_{0m} \\ + c_9 s^2 \Psi_m + c_{10} s^2 W_m = 0, \\ -r^2 d_1 \Theta_{1m} - r^2 d_2 \Theta_{2m} + d_3 s \Theta_{1m} + d_4 s \Theta_{2m} \\ - r d_5 s U_{0m} - r d_6 s \Psi_m - r^2 d_7 s W_m + (2d_9/rs) q^+ = 0, \\ -r^2 e_1 \Theta_{1m} - r^2 e_2 \Theta_{2m} + e_3 \Theta_{2m} + e_4 s \Theta_{1m} + e_5 s \Theta_{2m} \\ - r e_6 s U_{0m} - r e_7 s \Psi_m - r^2 e_8 s W_m + (2e_{10}/rs) q^+ = 0. \end{aligned} \quad (18)$$

where  $s$  is the Laplace transform parameter and

$$\begin{aligned} U_{0m} &= L[\bar{u}_{0m}], \\ \Psi_m &= L[\bar{\psi}_m], \\ W_m &= L[\bar{w}_m], \\ \Theta_{1m} &= L[\bar{\theta}_{1m}], \\ \Theta_{2m} &= L[\bar{\theta}_{2m}]. \end{aligned} \quad (19)$$

Thus, the solution of unknown variables in Eqs. (18) in the Laplace transformation domain can be given as

$$F_m(s) = \frac{Q_m(s)}{P_m(s)}. \quad (20)$$

where  $Q_m(s)$  and  $P_m(s)$  are polynomial functions of  $s$ . As an example, the lateral deflection function in the Laplace domain for coupled assumption is given as

$$W_m(s) = \frac{\delta(q_0 + q_2 s^2)}{s(p_0 + p_1 s + p_2 s^2 + p_3 s^3 + p_4 s^4 + p_5 s^5)} \quad (21)$$

where  $q$ 's,  $p$ 's and  $\delta$  are given in Appendix B. Carrying out the inverse Laplace transform of Eq. (20), the solution of unknown variables in time domain are obtained as [2,3]

$$f_m(t) = \sum_{j=1}^{n_p} \frac{Q_m(s_{p_j})}{P'_m(s_{p_j})} e^{s_{p_j} t} \quad (22)$$

where  $s_{p_j}$  are the roots of  $P_m(s)$  and  $n_p$  is the number of roots. Also, (') sign in superscript indicates derivative respect to  $s$ . According to Eqs. (16) and Eq. (22), the unknown variable functions are obtained in terms of space variable  $x$  and time  $t$ . As an example, the lateral deflection function can be given as

$$\begin{aligned} \bar{w}(\bar{x},\bar{t}) &= 2 \sum_{m=1,3,\dots}^{\infty} \bar{w}_m(m,\bar{t}) \sin(m\pi\bar{x}) \\ &= 2 \sum_{m=1,3,\dots}^{\infty} \sum_{j=1}^{n_p} \frac{\delta(q_0 + q_2 s_{p_j}^2)}{P'_w(s_{p_j})} e^{s_{p_j} \bar{t}} \sin(m\pi\bar{x}) \end{aligned} \quad (23)$$

$$\begin{aligned} P'_w(s_{p_j}) &= p_0 + 2p_1 s_{p_j} + 3p_2 s_{p_j}^2 + 4p_3 s_{p_j}^3 + \\ &5p_4 s_{p_j}^4 + 6p_5 s_{p_j}^5 \end{aligned}$$

## Results Discussion

To study the effect of lateral thermal shock on the beam with coupled thermoelastic assumption, an aluminum beam of length 0.25m and height 0.0022m is assumed. The material properties of aluminum are shown in Table 1. The thermal boundary conditions at the ends of the beam are assumed to be ambient temperature  $T_0 = 293K$ . The upper side of the beam is subjected to a step function thermal shock while the lower side is insulated.

**Table 1.** Material properties of aluminum

$E = 70\text{Gpa}$	$\rho = 2707\text{ kg/m}^3$
$G = 26\text{Gpa}$	$K = 204\text{ W/m}^0\text{K}$
$\alpha = 23 \times 10^{-6}\text{ 1/}^0\text{K}$	$c_v = 903\text{ J/kg}^0\text{K}$

Figure 2 shows temperature change history between upper and lower surfaces at the midpoint of the heated beam for the uncoupled assumption reported by [2] for Euler-Bernoulli beam and the present study. Due to the applied step function thermal shock, the beam temperature peaks to a maximum value, and then diffuses during the time. Close agreement is observed between the two studied for temperature histories. Figure 3 shows the midpoint lateral deflection history of Euler-Bernoulli beam with uncoupled assumptions reported by [2] and the present study. Due to the applied thermal shock, beam vibrated. It is observed that the maximum lateral deflection and the amplitude of vibration for Euler-Bernoulli beam theory are larger than that obtained using the higher-order shear deformation theory.

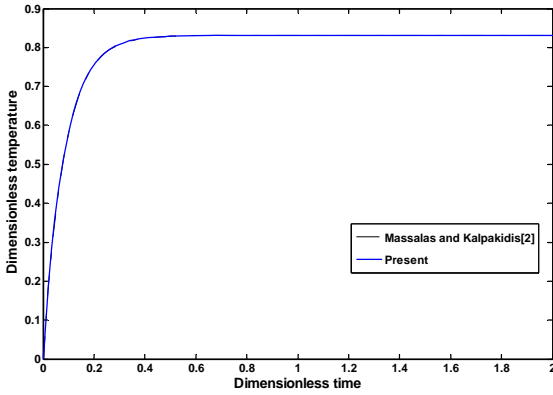


**Figure 2.** Temperature change history between upper and lower surfaces at the midpoint of the beam.

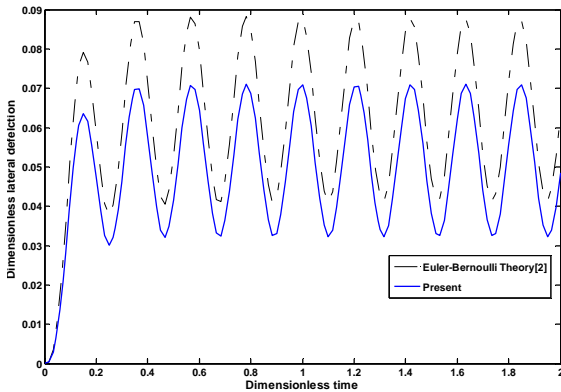


**Figure 3.** Lateral deflection history at the midpoint of the beam.

According to Eqs. (16) and Eq. (22) and considering  $m=1$ , the numerical functions of dimensionless lateral deflection  $w$  and dimensionless temperature change  $\theta_2$  are obtained at the midpoint of the beam for coupled and uncoupled assumptions.

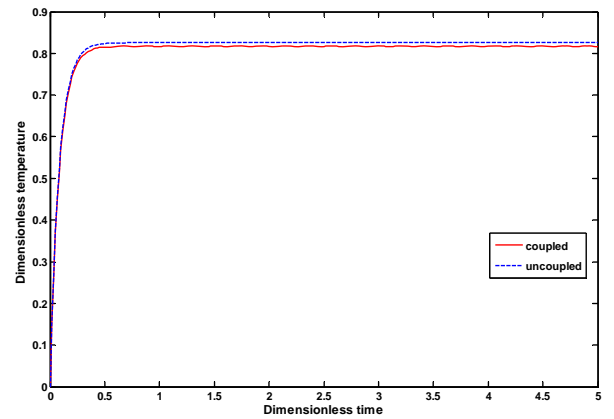
$$\begin{aligned} \bar{w}_{uncoupled}(0.5, \bar{t}) &= 0.0515966 - 0.0443701e^{(-12.001 \bar{t})} \\ &- 7.29508 \times 10^{-3} \cos(29.5735 \bar{t}) \\ &- 1.79773 \times 10^{-2} \sin(29.5735 \bar{t}) \\ &+ 1.39251 \times 10^{-18} \cos(261373 \bar{t}) \\ &+ 3.03286 \times 10^{-14} \sin(261373 \bar{t}) \end{aligned} \quad (24)$$

and the coupled one as

$$\begin{aligned} \bar{w}_{coupled}(0.5, \bar{t}) &= 0.0515966 - 0.0443789e^{(-11.963 \bar{t})} \\ &- 7.21772 \times 10^{-3} \cos(29.6193 \bar{t})e^{(-0.01856 \bar{t})} \\ &- 1.79297 \times 10^{-2} \sin(29.6193 \bar{t})e^{(-0.01856 \bar{t})} \\ &+ 1.39251 \times 10^{-18} \cos(261373 \bar{t})e^{(-5.3816 \times 10^{-6} \bar{t})} \\ &+ 3.03286 \times 10^{-14} \sin(261373 \bar{t})e^{(-5.3816 \times 10^{-6} \bar{t})} \\ \bar{\theta}_{2coupled}(0.5, \bar{t}) &= 0.817317 - 0.818029e^{(-11.963 \bar{t})} \\ &+ 7.1171 \times 10^{-4} \cos(29.6193 \bar{t})e^{(-0.01856 \bar{t})} \\ &+ 1.85603 \times 10^{-2} \sin(29.6193 \bar{t})e^{(-0.01856 \bar{t})} \\ &+ 3.09111 \times 10^{-15} \cos(261373 \bar{t})e^{(-5.3816 \times 10^{-6} \bar{t})} \\ &+ 3.36663 \times 10^{-11} \sin(261373 \bar{t})e^{(-5.3816 \times 10^{-6} \bar{t})} \end{aligned} \quad (25)$$

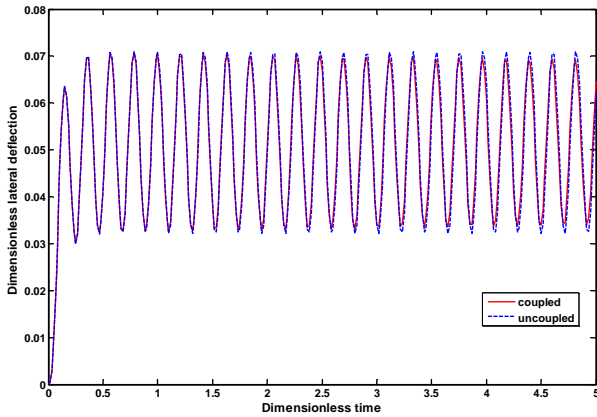
It is found from Eqs. (24) and (25) that the dimensionless lateral deflection  $w$  has the same frequency of oscillations as the dimensionless temperature change  $\theta_2$ . Also, no distinguishable difference is observed in the frequency of oscillations for the coupled and uncoupled solutions.

According to Eqs. (24) and (25), the temperature change history between upper and lower surfaces at the midpoint of the heated beam for the uncoupled and coupled assumptions is shown in Figure 4. It can be seen from Figure 4 that the temperature is vibrating with small amplitude when the coupling between the strain and temperature fields is taken into account.

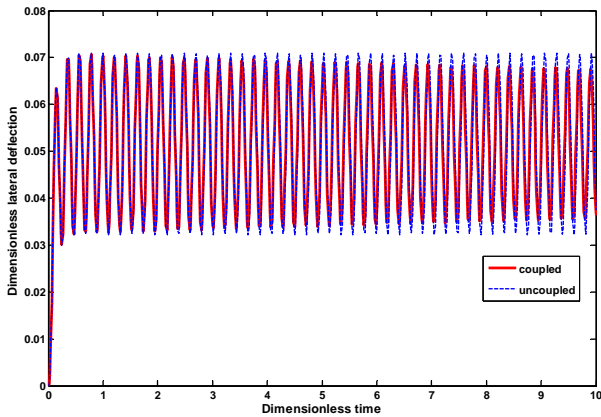


**Figure 4.** Temperature change history between upper and lower surfaces at the midpoint of the beam for coupled and uncoupled solutions.

According to Eqs. (24) and (25), Figure 5 shows the midpoint lateral deflection history for the uncoupled and coupled assumptions. It can be seen from Figure 5 that the vibration of the beam decays as time increases, when the coupling between the strain and temperature fields is taken into account. Also, no significant difference is seen in both coupled and uncoupled solutions. Since the vibrations of the beam for the uncoupled and coupled solutions is hardly distinguished from the curves in Figure 5, the difference between two solutions is shown for long time in Figure 6 to see the vibration decay caused by thermoelastic damping and the couple effect.



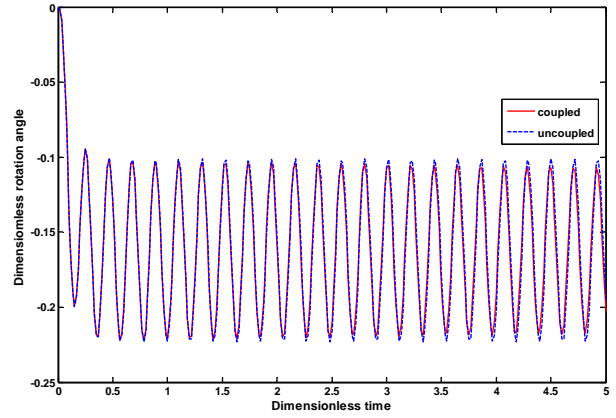
**Figure 5.** Lateral deflection history at the midpoint of the beam for coupled and uncoupled solutions.



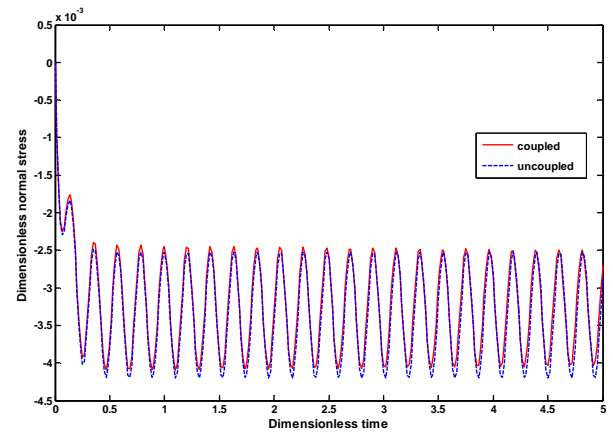
**Figure 6.** Lateral deflection history at the midpoint of the beam for coupled and uncoupled solutions.

Figure 7 shows the history of maximum rotation angle of the cross-section with respect to the longitudinal axis for the uncoupled and coupled assumptions. It can be seen from Figure 7 that due to the coupling effect, the rotation angle of the cross-section, similar to the lateral deflection, decays as time increases.

Figure 8 shows the normal stress history at the midpoint of the beam on the upper surface for the uncoupled and coupled solutions. As seen, it decreases with respect to time for coupled solution. Also, It is observed that the maximum normal stress for the uncoupled assumption is larger than that obtained using the coupled solution. Figure 9 shows the maximum shear stress history of the beam for the uncoupled and coupled assumptions. As shown in Figure 9, the amplitude of shear stress oscillations decreases slightly because of the coupling effect.



**Figure 7.** History of maximum rotation angle of the cross-section with respect to the longitudinal axis for the uncoupled and coupled solutions.



**Figure 8.** Normal stress history at the midpoint of the beam on the upper surface for the uncoupled and coupled solutions.

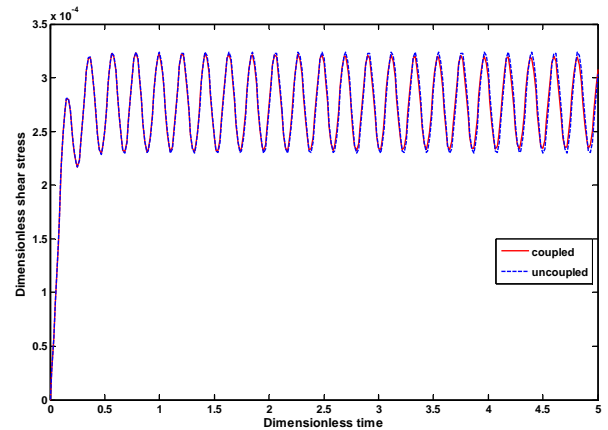


**Figure 9.** Maximum shear stress history of the beam for the uncoupled and coupled solutions.

## Conclusions

In the present paper, the coupled thermoelasticity of a beam based on the higher-order shear deformation theory is investigated. The beam is subjected to a thermal shock of step function on the upper side while the lower side is insulated. Boundary conditions of the beam are assumed to be simply supported with the ends of the beam at ambient temperature. To solve the problem, the finite Fourier transformation is used. Moreover, to treat the time dependency, the Laplace transform technique is applied. The inverse of Laplace

transform is carried out analytically.

Results show the temperature peaks to a maximum value, and then remains at this value. Temperature is vibrating with small amplitudes due to the coupling effect. It is concluded that the maximum lateral deflection and the amplitude of vibration, for the Euler-Bernoulli beam theory, are larger than that obtained using the higher-order shear deformation theory.

Since the flexural theory of thermoelasticity is used, the stress wave is not observed across the beam thickness. The oscillations of the lateral deflection, axial stress and shear stress are, however, observed. Moreover, it is generally concluded that there is no significant difference between the coupled and uncoupled solutions. However, the effect of coupling is similar to damping. The vibration of the beam decays as time increases when the coupling between the strain and temperature fields is taken into account.

### List of Symbols

$c_v$	specific heat
$E$	modulus of elasticity
$G$	shear modulus
$k$	thermal conductivity
$\kappa$	thermal diffusivity
$q$	heat flux
$u$	axial displacement
$w$	lateral deflection
$\alpha$	linear thermal expansion
$\varepsilon$	strain
$\theta$	temperature change
$\rho$	density
$\sigma$	stress
$\psi$	rotation angle

### References

- [1] McQuillen, E.J. and Brull, M.A., 1970, "Dynamic thermoelastic response of cylindrical shell ", *J. Applied Mechanics*, **37**, 661-670.
- [2] Massalas, C.V. and Kalpakidis, V.K., 1983, "Coupled thermoelastic vibration of a simply supported beam ", *J. Sound and Vibration*, **88**, 425-429.
- [3] Massalas, C.V. and Kalpakidis, V.K., 1984, "Coupled thermoelastic vibration of a Timoshenko beam ", *Lett. Appl. Engng Sci.*, **22**, 459-465.
- [4] Eslami, M.R. and Vahedi, H., 1988, "Coupled thermoelasticity beam problems ", *AIAA J.*, **27**, 662-665.
- [5] Maruthi, D.R. and Sinha, P.K., 1997, "Finite element coupled thermostructural analysis of composite beams ", *Computers and Structures*, **63**, 539-549.
- [6] Manoach, E. and Ribeiro, P., 2004, "Coupled thermoelastic large amplitude vibrations of Timoshenko beams ", *J. Mechanical Science*, **46**, 1589-1606.
- [7] Sun, Y., Fang, D. and Soh, A.K., 2006, "thermoelastic damping in micro-beams resonators ", *Int. J. Solids and Structures*, **43**, 3213-3229.
- [8] Reddy J. N., 2002, *Energy Principles and Variational Methods in Applied Mechanics*, New York: John Wiley & Sons.

### Appendix A

$$\begin{aligned}
 A_1 &= \int E dz \\
 A_2 &= \int E z dz + \int -c'E z^3 dz \\
 A_3 &= \int -c'E z^3 dz \\
 A_4 &= \int -E \alpha dz \\
 A_5 &= \int -E \alpha \frac{z}{h} dz \\
 A_6 &= -I_0 \\
 A_7 &= -J_1 \\
 A_8 &= c'I_3 \\
 B_1 &= \int c'E z^3 dz \\
 B_2 &= \int G dz - 6c' \int G z^2 dz + 9c'^2 \int G z^4 dz \\
 B_3 &= c' \int E z^4 dz - c'^2 \int E z^6 dz \\
 B_4 &= \int G dz - 6c' \int G z^2 dz + 9c'^2 \int G z^4 dz \\
 B_5 &= -c'^2 \int E z^6 dz \\
 B_6 &= \int -E \alpha z^3 dz \\
 B_7 &= \int -E \alpha \frac{z^4}{h} dz \\
 B_8 &= -c'I_3 \\
 B_9 &= -J_4 \\
 B_{10} &= -I_0 \\
 B_{11} &= c'^2 I_6 \\
 C_1 &= \int E z dz - c' \int E z^3 dz \\
 C_2 &= \int G dz - 6c' \int G z^2 dz + 9c'^2 \int G z^4 dz \\
 C_3 &= \int E z^2 dz - 2c' \int E z^4 dz + c'^2 \int E z^6 dz \\
 C_4 &= \int G dz - 6c' \int G z^2 dz + 9c'^2 \int G z^4 dz \\
 C_5 &= -c' \int E z^4 dz + c'^2 \int E z^6 dz \\
 C_6 &= \int -E \alpha z dz + c' \int E \alpha z^3 dz \\
 C_7 &= \int -E \alpha \frac{z^2}{h} dz + c' \int E \alpha \frac{z^4}{h} dz \\
 C_8 &= -J_1 \\
 C_9 &= -K_2 \\
 C_{10} &= J_4 \\
 D_1 &= \int K dz \\
 D_2 &= \int K \frac{z}{h} dz \\
 D_3 &= \int -\rho c dz \\
 D_4 &= \int -\rho c \frac{z}{h} dz
 \end{aligned}$$

$$D_5 = \int -E \alpha T_0 dz$$

$$D_6 = \int -E \alpha z T_0 dz + c' \int E \alpha z^3 T_0 dz$$

$$D_7 = c' \int E \alpha z^3 T_0 dz$$

$$D_8 = -1$$

$$D_9 = 1$$

$$E_1 = \int K z dz$$

$$E_2 = \int K \frac{z^2}{h} dz$$

$$E_3 = \int -\frac{K}{h} dz$$

$$E_4 = \int -\rho c z dz$$

$$E_5 = \int -\rho c \frac{z^2}{h} dz$$

$$E_6 = \int -E \alpha z T_0 dz$$

$$E_7 = \int -E \alpha z^2 T_0 dz + c' \int E \alpha z^4 T_0 dz$$

$$E_8 = c' \int c_1 E \alpha z^4 T_0 dz$$

$$E_9 = \frac{h}{2}$$

$$E_{10} = \frac{h}{2}$$

$$p_3 = (b_7 b_{11} e_7 - b_3 b_{11} e_5) r^5 + (b_9 c_5 e_5 + b_7 c_9 e_8 + b_{11} c_7 e_7 + b_3 c_{10} e_5 - b_7 c_{10} e_7 - b_{11} c_3 e_5 - b_5 c_9 e_5 - b_9 c_7 e_8) r^4 + b_2 b_{11} e_5 r^3 + (b_{11} c_2 e_5 + b_4 c_9 e_5 + b_{10} c_3 e_5 - b_9 c_4 e_5 - b_{10} c_7 e_7 - b_2 c_{10} e_5) r^2 - b_{10} c_2 e_5$$

$$p_4 = -b_9 b_{11} e_2 r^5 + (b_9 c_{10} e_2 - b_{11} c_9 e_2) r^4 - b_9 b_{11} e_3 r^3 + (b_{10} c_9 e_2 + b_{11} c_9 e_3 - b_9 c_{10} e_3) r^2 - b_{10} c_9 e_3$$

## Appendix B

$$\delta = 2q^+ r e_{10}$$

$$q_0 = b_7 c_2 - b_2 c_7 + r^2 (b_3 c_7 - b_7 c_3)$$

$$q_2 = b_7 c_9 - b_9 c_7$$

$$p_0 = (b_3 c_5 e_2 - b_5 c_3 e_2) r^8 + (b_5 c_2 e_2 + b_4 c_3 e_2 + b_5 c_3 e_3 - b_3 c_5 e_3 - b_3 c_4 e_2 - b_2 c_5 e_2) r^6 + (b_3 c_4 e_3 + b_2 c_5 e_3 + b_2 c_4 e_2 - b_4 c_2 e_2 - b_5 c_2 e_3 - b_4 c_3 e_3) r^4 + (b_4 c_2 e_3 - b_2 c_4 e_3) r^2$$

$$p_1 = (b_5 c_3 e_5 + b_3 c_7 e_8 + b_7 c_5 e_7 - b_3 c_5 e_5 - b_7 c_3 e_8 - b_5 c_7 e_7) r^6 + (b_2 c_5 e_5 + b_3 c_4 e_5 + b_7 c_2 e_8 + b_4 c_7 e_7 - b_4 c_3 e_5 - b_7 c_4 e_7 - b_5 c_2 e_5 - b_2 c_7 e_8) r^4 + (b_4 c_2 e_5 - b_2 c_4 e_5) r^2$$

$$p_2 = b_3 b_{11} e_2 r^7 + (b_5 c_9 e_2 + b_{11} c_3 e_2 - b_3 c_{10} e_2 - b_9 c_5 e_2) r^6 + (-b_3 b_{11} e_3 - b_2 b_{11} e_2) r^5 + (b_9 c_5 e_3 + b_3 c_{10} e_3 + b_9 c_4 e_2 + b_2 c_{10} e_2 - b_4 c_9 e_2 - b_5 c_9 e_3 - b_{11} c_3 e_3 - b_{11} c_2 e_2 - b_{10} c_3 e_2) r^4 + b_2 b_{11} e_3 r^3 + (b_{11} c_2 e_3 + b_{10} c_3 e_3 + b_{10} c_2 e_2 + b_2 c_{10} e_2 + b_4 c_9 e_3 - b_2 c_{10} e_3 - b_9 c_4 e_3) r^2 - b_{10} c_2 e_3$$